

CHAPTER 3: PHOTOREDUCTION OF Pt(POP-BF₂)⁴⁻

To quantitatively probe the excited-state oxidizing power of Pt(pop-BF₂)⁴⁻, a series of luminescence quenching experiments was carried out.

3.1 Analysis of quenching

Quenching in a chemical sense may be described as any process which decreases the fluorescence intensity of a substance. There are two basic types of quenching: static and dynamic. Both static and dynamic (diffusional) quenching require physical contact between the fluorophore and the quencher.¹

Static quenching occurs when a nonfluorescent ground-state complex containing both fluorophore and quencher exists prior to excitation of the fluorophore; this is often achieved by the formation of ion pairs utilizing oppositely charged quenchers and fluorophores. When such a complex absorbs light, it returns to the ground state without emitting a photon. In the case of static quenching, the dependence of fluorescence intensity on quencher concentration may be derived by calculating the association constant for complex formation, K_s .¹

$$K_s = \frac{[F - Q]}{[F][Q]} \quad (1)$$

In equation (1), $[F - Q]$ is the concentration of the fluorophore-quencher complex, $[F]$ is the concentration of uncomplexed fluorophore, and $[Q]$ is the concentration of uncomplexed quencher. If the complex is nonfluorescent, then the fraction of remaining fluorescence F/F_0 is equivalent to the fraction of total fluorophores not complexed. As the total concentration of fluorophore is $[F]_0 = [F] + [F - Q]$, substitution into equation (1) and subsequent rearrangement yields equation (2):

$$\frac{F_0}{F} = 1 + K_s[Q] \quad (2)$$

Of particular importance is the fact that because static quenching stops a fraction of available fluorophores from emitting without affecting the remaining uncomplexed fluorophores, the fluorophore lifetime is unaffected and $\tau_0 = \tau$.

Dynamic, or diffusional, quenching occurs when the decrease in fluorescence intensity is caused by collisional encounters between fluorophore and quencher. As such, the fluorophore and quencher must diffuse together within the timeframe dictated by the excited state lifetime τ_0 . Collisional quenching is described by the Stern-Volmer equation:

$$\frac{F_0}{F} = 1 + k_q\tau_0[Q] = 1 + K_D[Q] \quad (3)$$

In equation (3), F_0 and F are the fluorescence intensities in the absence and presence of quencher, k_q is the bimolecular quenching constant, τ_0 is the lifetime of the fluorophore without quencher, $[Q]$ is the concentration of quencher and K_D is the Stern-Volmer quenching constant. As F_0/F is expected to have a linear dependence on $[Q]$, quenching data are typically presented as a plot of F_0/F versus $[Q]$; this yields a line with a y-intercept of 1 and a slope of K_D .¹ A linear Stern-Volmer plot is indicative of a single fluorophore, all of which are equally accessible to quencher molecules.

Inspection of equation (2) shows that static quenching behavior may also yield a linear relationship between F_0/F and $[Q]$. Therefore, in order to unambiguously assign a type of quenching behavior, the fluorescence lifetimes in the presence and absence of quencher (τ_0 and τ) must be measured.

3.2 Fluorophore lifetime measurements

The excitation of a fluorophore with an infinitely short pulse of light results in an initial population N_0 of fluorophores in the excited state. At any time t after the initial excitation, the number of excited molecules may be described as $N(t)$. As time passes, this population decays at a rate dependent on the emissive rate γ and the non-radiative decay rate k_{nr} :

$$\frac{dN(t)}{dt} = -(\gamma + k_{nr})N(t) \quad (4)$$

As $N(t = 0) = N_0$, equation (4) may be integrated to yield

$$N = N_0 e^{-t/\tau} \quad (5)$$

in which τ is the lifetime of the excited state. The fluorescence lifetime is generally defined to be the time required for the intensity to decay to $1/e$ of its original value; or,

$$\tau = \frac{1}{\gamma + k_{nr}} \quad (6)$$

Finally, the fluorescence intensity measured by an instrument, $F(t)$, is proportional to the excited state population:

$$N(t) \cong F(t) \quad (7)$$

Thus, the slope of a plot of $\log F(t)$ versus t will be $-1/\tau$.

3.3 Quenching of $^3[\text{Pt}(\text{pop-BF}_2)^4]^*$ phosphorescence

The excited-state lifetimes of the $[\text{Pt}(\text{pop-BF}_2)^4]$ singlet and triplet states were measured by Durrell and coworkers in 2012. The triplet state has a lifetime of $8.4 \mu\text{s}$ with an emission maximum at 512 nm; meanwhile, the singlet state has a lifetime of 1.6 ns with an emission maximum of 393 nm.² The length of the triplet lifetime affords ample time for diffusional quenching to occur. The

presence of diffusional quenching may be observed as a decrease in either luminescence lifetime or steady-state luminescence intensity at the triplet emission wavelength maximum of 512 nm. As shown in Figure 1, after the triplet excited state of $\text{Pt}(\text{pop-BF}_2)^4$ is produced following excitation with 355 nm light, it may return to the ground state either by emission of a photon or by reacting with an electron-transfer type quencher molecule to produce the oxidized quencher and reduced $\text{Pt}(\text{pop-BF}_2)^5$. The degree to which the nonemissive path is favored over the emissive pathway is demonstrated by the relative magnitude of the decrease in luminescence intensity. After quenching occurs, it is possible for the products to react to reform the reactants, Q and $\text{Pt}(\text{pop-BF}_2)^4$, provided that Q^+ does not decompose.

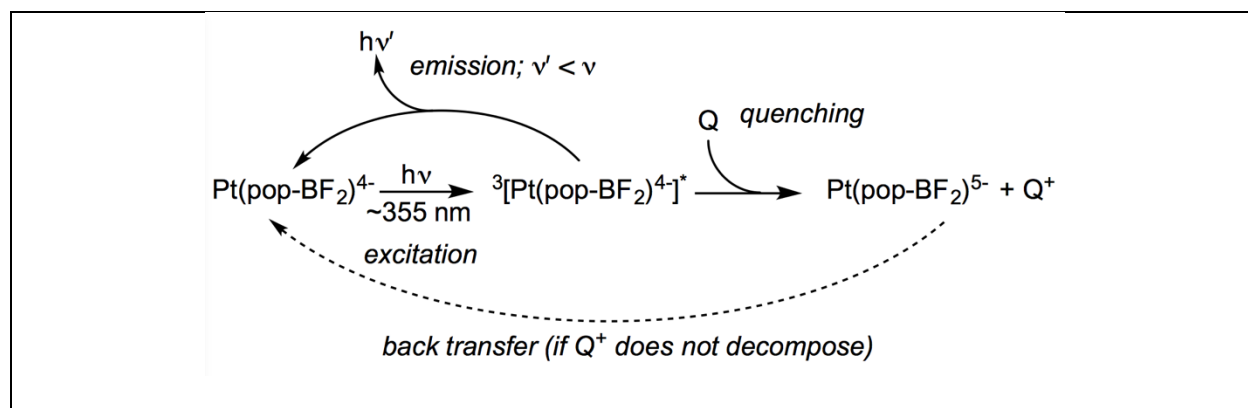
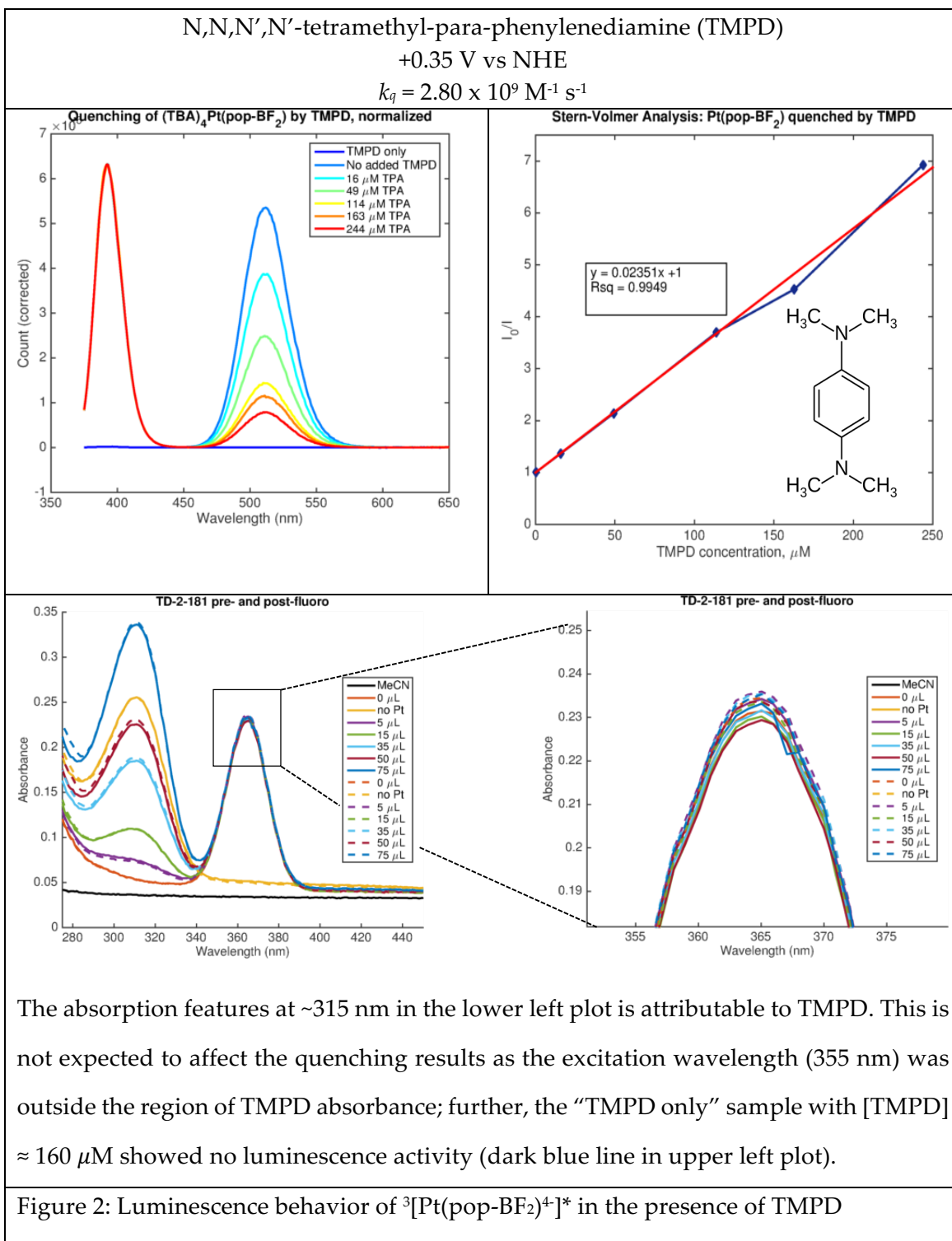


Figure 1: Dynamic (diffusional) reductive quenching scheme.

The excited-state behavior of $\text{Pt}(\text{pop})^4$ is well known and has been deeply investigated,³⁻¹² while that of $\text{Pt}(\text{pop-BF}_2)^4$ remains relatively unexplored.^{13,14} Furthermore, as yet the only extant data on the oxidizing power of $\text{Pt}(\text{pop-BF}_2)^4$ excited states are estimates based on spectral data (see Chapter 1).^{2,13,15} By tracking how the quenching rate of an emissive state changes based on the oxidation potential of the selected quencher molecule, a good estimate of the potential of the excited state may be obtained.¹⁶⁻¹⁸ As such, the emissive properties of $\text{Pt}(\text{pop-BF}_2)^4$ were studied in the presence of various organic amine quenchers. The specific amines used in this section were

chosen as quenchers because of their lack of absorption bands in the areas of Pt(pop-BF₂)⁴⁻ absorption, their ranges of oxidation potential, and their solubility in acetonitrile.¹⁴

Briefly, solutions of Pt(pop-BF₂)⁴⁻ of a fixed concentration (~10 μM) were prepared such that the total absorbance at the 355 nm excitation wavelength was between 0.05 and 0.1; these solutions were spiked with increasing concentrations of quencher and their steady-state luminescence profiles were recorded using fluorimetry. Quencher-only solutions were also prepared and analyzed to ensure that the quencher was not luminescing due to excitation from the 355 nm probe wavelength. The singlet emission intensity was measured and used as a normalization factor, as the 1.6 ns lifetime of the singlet state hampers it from participating in diffusional quenching; furthermore, noted deviation in the singlet-state intensity from spectrum to spectrum was within instrument error.² Finally, the solutions were monitored by UV-Vis spectroscopy during the course of the experiment to check for any possible decomposition; no such decomposition was observed. Stern-Volmer type quenching behavior was observed, and values for k_q were calculated for each quencher by plotting I_0/I (referred to as F_0/F in the equations of section 3.1) vs $[Q]$. Results are summarized in Figure 2, Figure 3, and Figure 4.



4-dimethylaminopyridine (DMAP)

+1.1 V vs NHE

$$k_q = 5.51 \times 10^8 \text{ M}^{-1} \text{ s}^{-1}$$

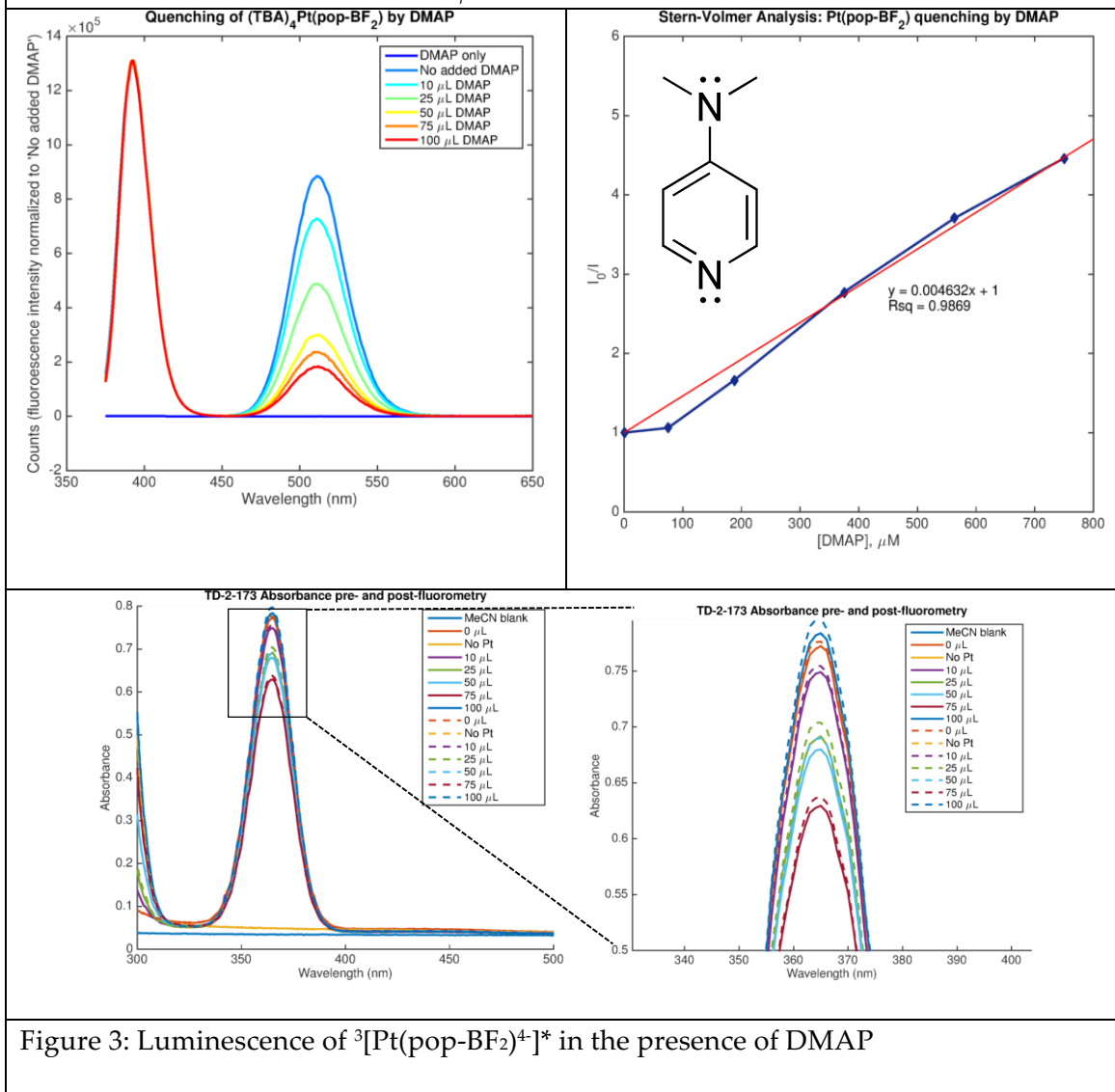
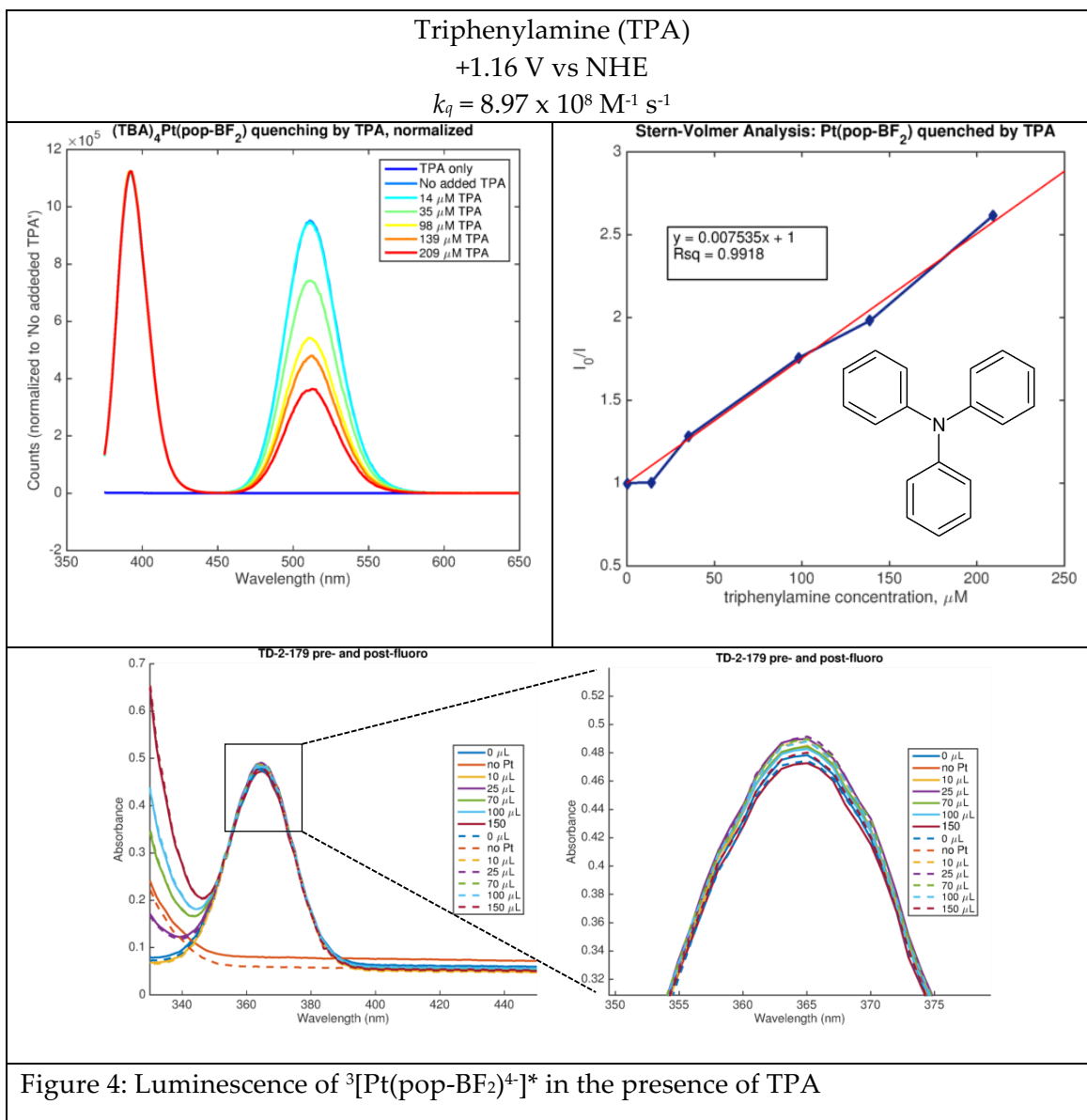


Figure 3: Luminescence of ${}^3[\text{Pt}(\text{pop-BF}_2)_4]^*$ in the presence of DMAP



The data obtained for these three quenchers demonstrate that the rate of quenching of the triplet state roughly tracks with the oxidation potential of the selected quencher; that is, when a quencher is easier to oxidize, the quenching rate increases. Data with more quenchers as well as additional trials with these three quenchers are needed to confirm the exact excited state potential of ${}^3[\text{Pt}(\text{pop-BF}_2)_4]^*$, but it is possible that Marcus-type behavior will be observed for $\text{Pt}(\text{pop-BF}_2)_5^-$

is likely due to a second-order dependence on quencher concentration, as diffusional and static quenching are both possible decay pathways. Such deviations from linearity, demonstrating concavity toward the y-axis, are well-documented in the literature as being ascribable to a combination of static and dynamic quenching.¹

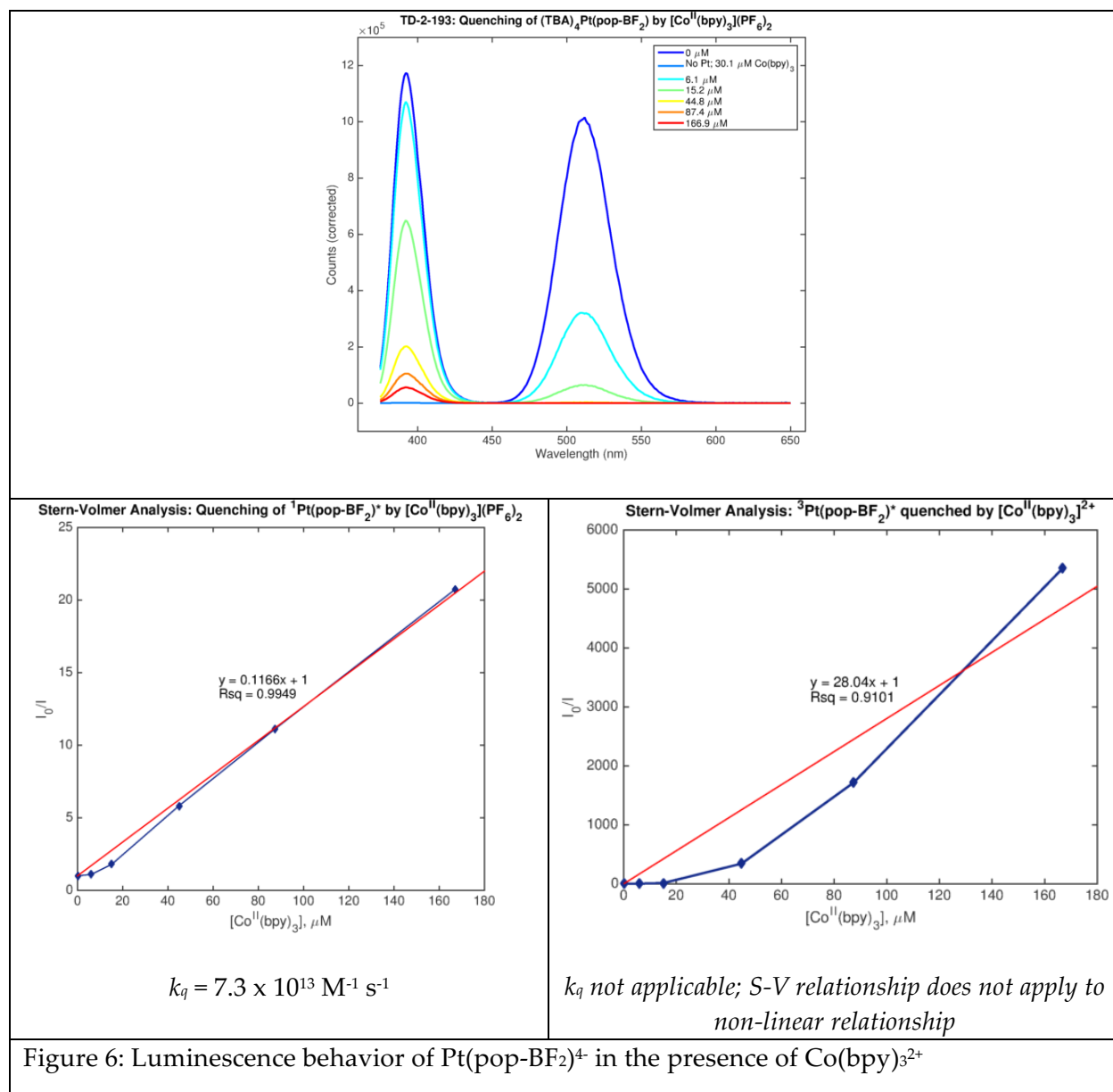
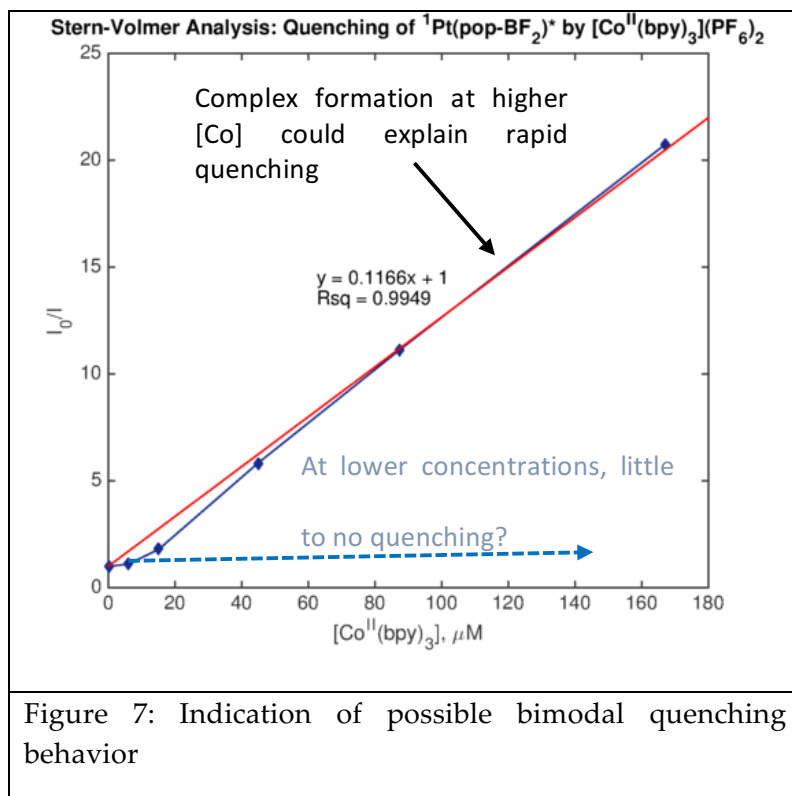


Figure 6: Luminescence behavior of Pt(pop-BF₂)₄⁺ in the presence of Co(bpy)₃²⁺

A putative singlet quenching rate exceeding $10^{13} \text{ M}^{-1} \text{ s}^{-1}$ was also calculated, seemingly ruling out the possibility of a wholly diffusional quenching mechanism given that the diffusion limit in acetonitrile is on the order of $10^{11} \text{ M}^{-1} \text{ s}^{-1}$. However, close investigation of the plot of I_0/I vs



$[\text{Q}]$ indicates a very slight deviation from linearity at lower concentrations. A possible explanation for this deviation could be that at low $[\text{Q}]$ there is little to no quenching, as the singlet lifetime is too short to allow for diffusional quenching and $[\text{Q}]$ could be too low to create a sizable population of quencher-

fluorophore complexes. Contrastingly, at high $[\text{Q}]$, rapid quenching (i.e. quenching rates in excess of the diffusion limit) could be attributed to static quenching behavior resulting from the favored formation of quencher-fluorophore complexes (Figure 7).

In an effort to further illuminate this behavior, quencher concentrations were lowered to $<20 \mu\text{M}$ to attempt to disfavor fluorophore-quencher complex formation and to add more data points to the plot in Figure 7. However, with the additional data at lower concentrations, the deviation from linearity was even more distinct for both the singlet and triplet states (Figure 8).

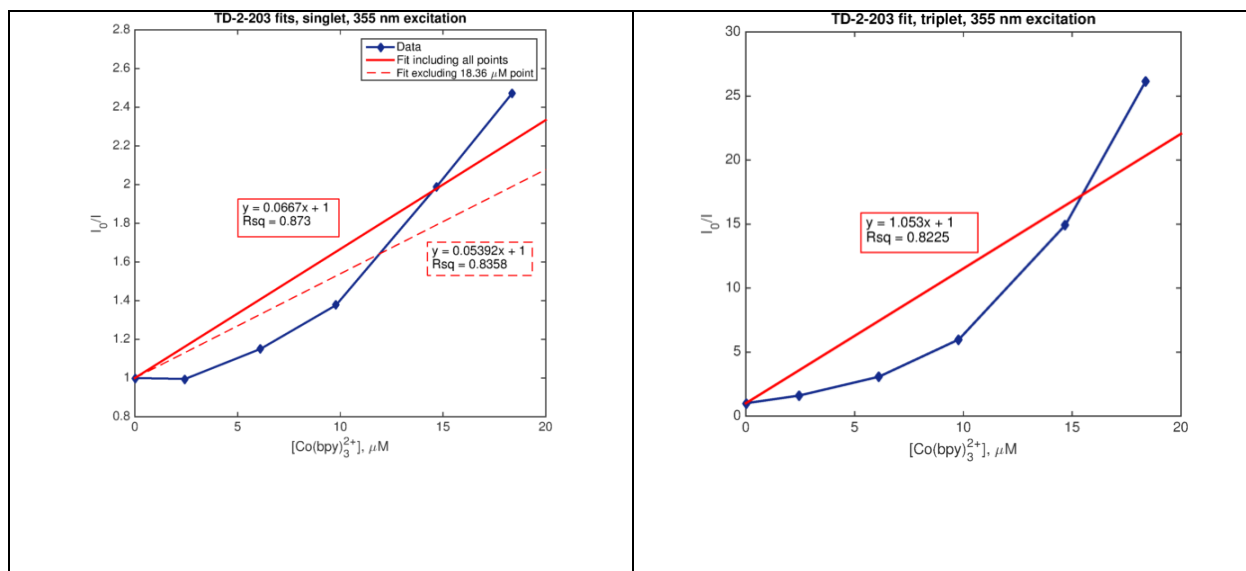


Figure 8: Substantial quenching of Pt(pop-BF₂)⁴⁺ singlet and triplet emission continues at low values of [Q]

Furthermore, the additional data points taken at lower concentrations follow the same pattern observed previously (Figure 9).

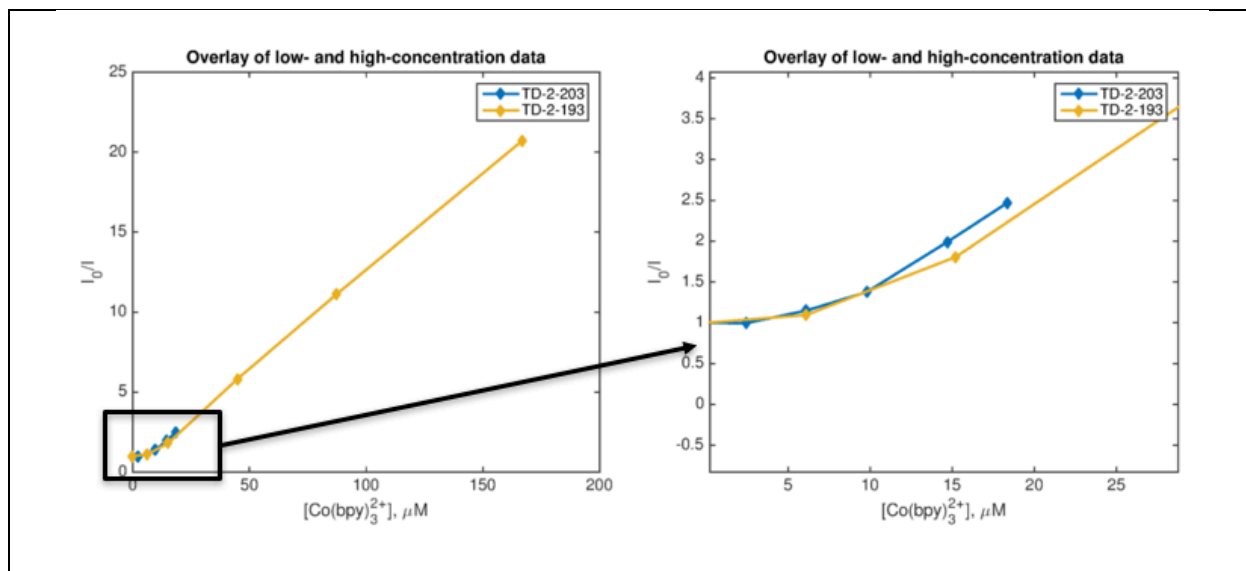
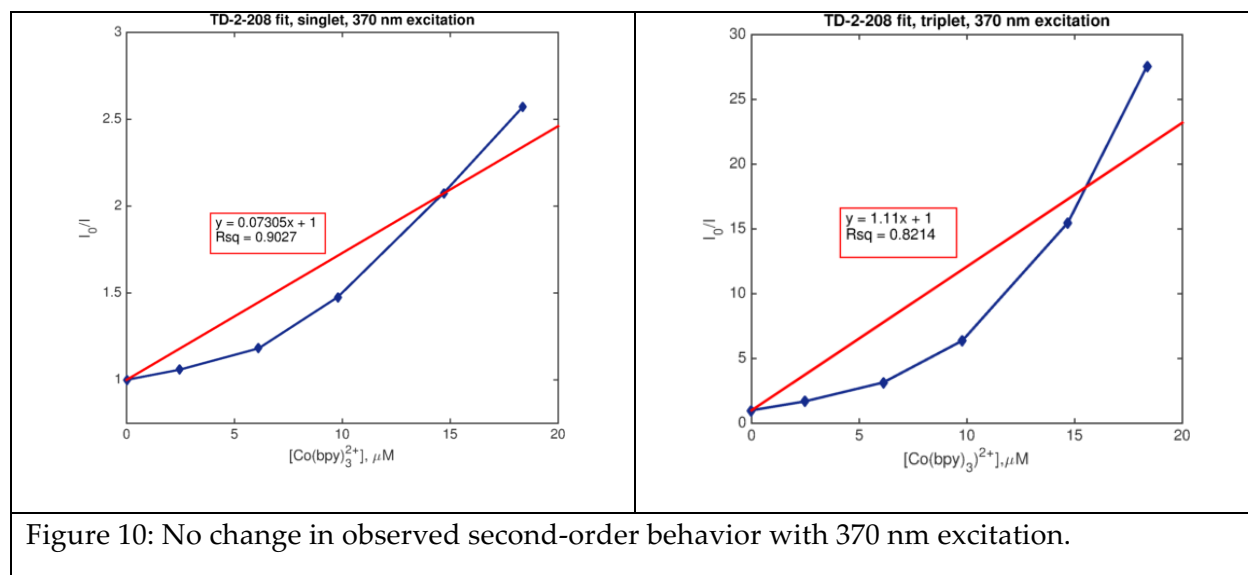


Figure 9: Overlay of quenching data obtained with [Q] = 0 – 170 μM (yellow) and [Q] = 0 – 20 μM (blue).

Finally, the excitation wavelength was moved to 370 nm to further reduce the very limited possibility of emission from the Co^{II} complex, which has an absorbance maximum at 305 nm ($\epsilon \approx 63,000 \text{ L mol}^{-1} \text{ cm}^{-1}$). The red-shift in excitation wavelength also had no effect on the quenching behavior (Figure 10), which is not particularly surprising given the Co^{II} complex's molar absorptivity constant of $<6000 \text{ L mol}^{-1} \text{ cm}^{-1}$ at 355 nm.

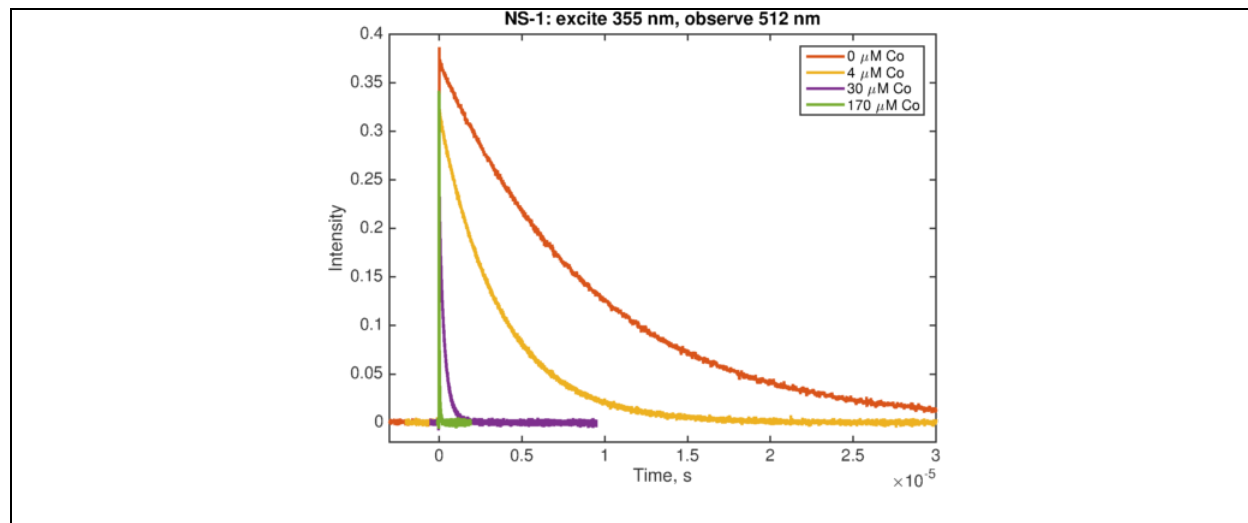


The diffusion rate limit in acetonitrile is on the order of $10^{10} - 10^{11} \text{ M}^{-1} \text{ s}^{-1}$,¹ so the k_q 's calculated for the singlet cannot be attributed solely to diffusional quenching. As a decrease in the emission intensity of the singlet was nevertheless observed in the presence of $\text{Co}(\text{bpy})_3^{2+}$, the quenching behavior must be attributed at least in part to non-diffusional energy and/or electron transfer between $^1[\text{Pt}(\text{pop-BF}_2)^4]^*$ and $[\text{Co}(\text{bpy})_3]^{2+}$. Steady-state techniques are insufficient to analyze this type of behavior; time-resolved experiments were undertaken.

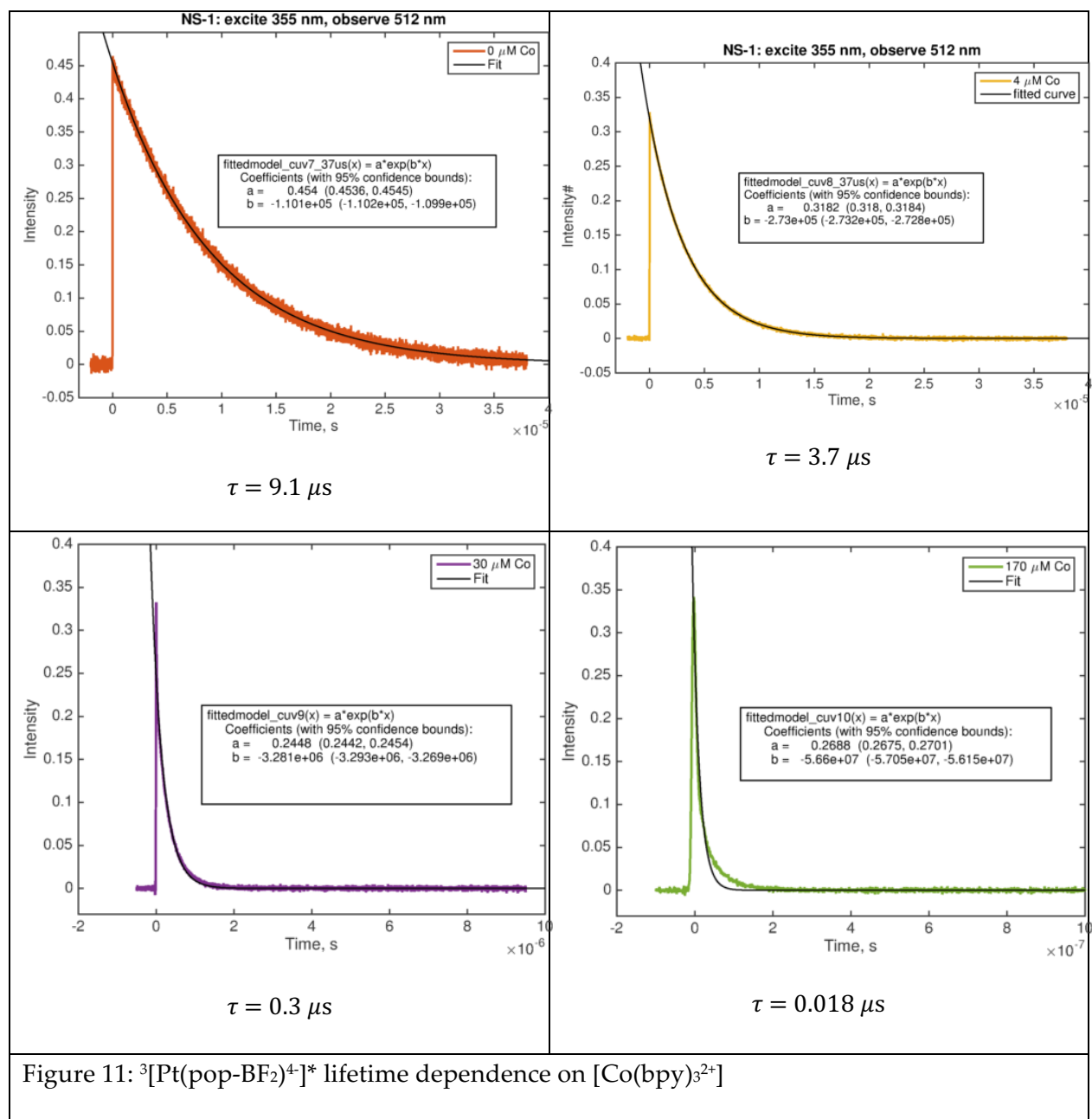
3.4.1 Time-resolved analysis: $^1[\text{Pt}(\text{pop-BF}_2)_4]^*$ and $^3[\text{Pt}(\text{pop-BF}_2)_4]^*$ luminescence quenching by $\text{Co}(\text{bpy})_3^{2+}$

As described in 3.3, solutions of $\text{Pt}(\text{pop-BF}_2)_4$ ($\sim 8 \mu\text{M}$) in acetonitrile were prepared and spiked with $(\text{Co}(\text{bpy})_3)^{2+}$ to yield quencher concentrations from 0 – 170 μM . Absorbance spectra were recorded before and after the experiment to monitor for compound decomposition.

Using 355 nm excitation, luminescence decay spectra were recorded at 512 and 400 nm (the approximate emission maxima of the triplet and the singlet, respectively).ⁱ The intensity decays were fitted to mono- or bi-exponential equations, as appropriate, and values for the excited-state lifetimes were calculated (see 3.2 for background). The lifetime of the triplet state decreased from an initial value of 9.1 μs without quencher to 0.018 μs when $[\text{Q}] = 170 \mu\text{M}$. Decay traces and fitting equations are shown in Figure 11.



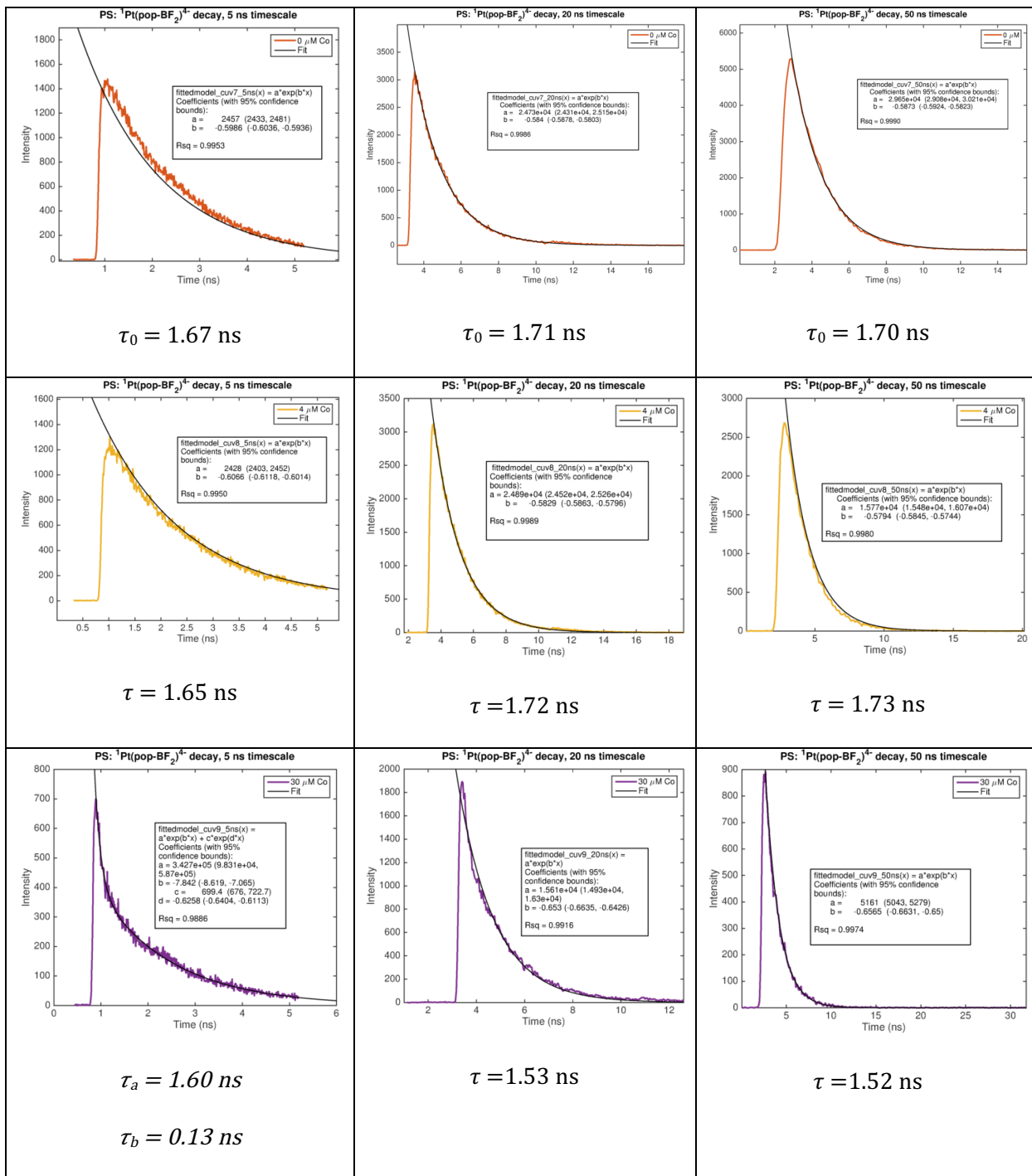
ⁱ The time-resolved data in section 3.4.1 were collected with the kind assistance of Oliver S. Shafaat.

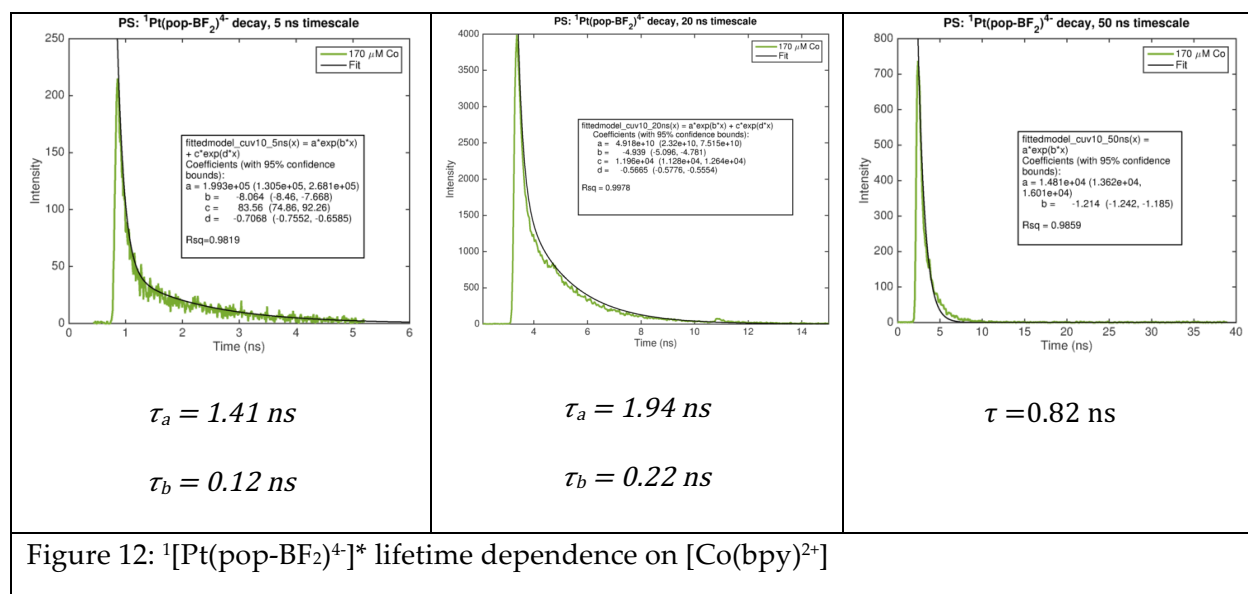


The behavior of the singlet was also investigated; data collection windows from 5 to 50 ns were utilized so as to record both the early- and late-times behavior with sufficient resolution. These decay traces as well as the fitting equations and calculated lifetimes are shown in Figure 12. The majority of the spectra were described well by a single-term exponential; however, others required the application of a second exponential term to acquire appropriate fitting equations. Lifetimes obtained from these biexponential fits are italicized in Figure 12. If one considers only

the data sets which could be reasonably described by a simple exponential decay, the lifetime for $^1[\text{Pt}(\text{pop-BF}_2)^4]^*$ with $4 \mu\text{M}$ $[\text{Co}(\text{bpy})_3^{2+}]$ was nearly identical ($\tau \approx 1.65 - 1.73 \text{ ns}$) to the unquenched τ_0 value of $1.67 - 1.70 \text{ ns}$. When $[\text{Co}(\text{bpy})_3^{2+}]$ increased to $30 \mu\text{M}$, the singlet lifetime decreased measurably to $\approx 1.55 \text{ ns}$. If the only quenching mechanism in action is static quenching, τ should equal τ_0 . A possible explanation is that for $[\text{Co}(\text{bpy})_3^{2+}] \lesssim 30 \mu\text{M}$, only static quenching is at work. When $[\text{Co}(\text{bpy})_3^{2+}]$ increases beyond that, complex formation may no longer be favored as proscribed by K_S , equation (1). This could occur, for instance, if $[\text{Co}(\text{bpy})_3^{2+}] \gg [\text{Pt}(\text{pop-BF}_2)^4]$. If complex formation is not favored and uncomplexed quencher still remains in solution, that excess quencher could facilitate diffusional quenching.

While it is unlikely that quencher and fluorophore could diffuse over long distances in the span of less than two nanoseconds, it is possible to have quencher and fluorophore close enough to each other at the time of excitation to cause near-instantaneous quenching.¹ This “sphere of action”-type behavior implicates a more complex quenching mechanism involving different degrees of static and diffusional quenching depending on the quencher concentration. To fully deconvolute the behavior, more data are needed; a potential analytical scheme is presented in section 3.5. Repeating the experiments described in this section with a broader range of quencher concentrations would provide needed information about exactly when τ begins to deviate from τ_0 . Furthermore, investigating the effects of temperature and solvent choice on the fluorophore-quencher interaction would allow the use of more accurate calculations that account for diffusional and static quenching behavior simultaneously.¹





Another possible contributing factor to the somewhat puzzling luminescence behavior is sample decomposition, which was unfortunately noted over the course of these laser experiments (Figure 13). The right-hand plot in Figure 13 shows the absorption maximum of $\text{Pt}(\text{pop-BF}_2)_4^+$; decreases in absorption intensity are noted for all samples over the course of the experiment. The full trace on the left additionally shows significant changes in absorption below 300 nm, where bands for both $\text{Pt}(\text{pop-BF}_2)_4^+$ and $\text{Co}(\text{bpy})_2^{2+}$ typically present. The composition of the samples undoubtedly changed during the experiment; the effects of those changes on the luminescence properties are unknown.

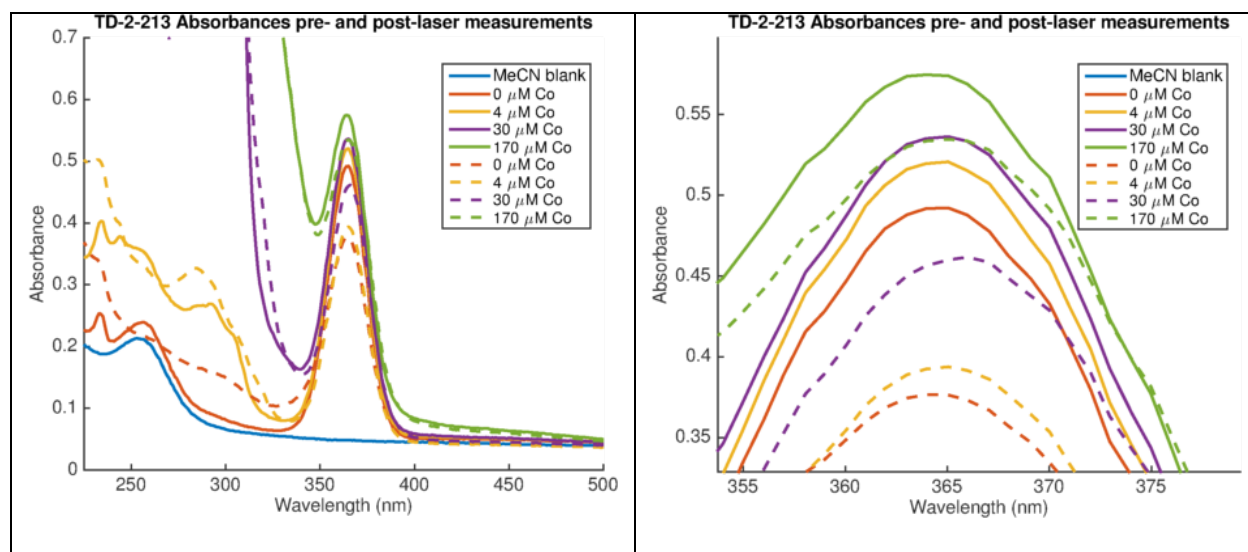


Figure 13: Absorbance spectra of samples before (solid line) and after (dashed line) laser experiments.

3.5 Conclusions

In some instances, a fluorophore may be quenched both by collision with a quencher molecule and by complex formation with the same quencher. Given the presented data collected for the quenching of $^1[\text{Pt}(\text{pop-BF}_2)^4]^*$ and $^3[\text{Pt}(\text{pop-BF}_2)^4]^*$ by $\text{Co}(\text{bpy})_3^{3+}$ and the fact that neither purely diffusional nor purely static analytical techniques describe the behavior observed, it is likely that a more complex mechanism involving both static and dynamic quenching is at play. Such behavior is second-order in $[\text{Q}]$, which would also account for the upward curvature observed for the plots of I_0/I vs $[\text{Q}]$ presented in Figure 7 through Figure 10.

In these cases, a modified form of the Stern-Volmer equation may be applied:

$$\frac{F_0}{F} = (1 + K_D[\text{Q}])(1 + K_S[\text{Q}]) \quad (8)$$

As in the equations presented in section 3.1 and 3.2, K_D is the Stern-Volmer quenching constant ($K_D = k_q\tau_0$), K_S is the association constant for fluorophore-quencher complex formation, $[\text{Q}]$ is the

concentration of quencher, and F_0/F is the ratio of unquenched luminescence intensity to the observed luminescence intensity at any quencher concentration $[Q]$. The dynamic part of the observed quenching may be determined via lifetime measurements:

$$\frac{\tau_0}{\tau} = 1 + K_D[Q] \quad (9)$$

Combination of equations (8) and (9) yields the following relation:

$$\frac{F_0}{F} = \frac{\tau_0}{\tau_{[Q]}} (1 + K_S[Q]) \quad (10)$$

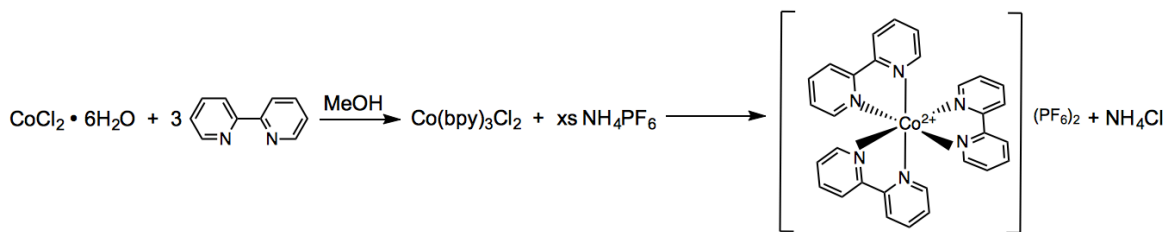
The analysis put forward in equation (10) requires a complete set of steady-state and time-resolved quenching data for a single set of samples; lifetimes and steady-state intensities must be acquired that the exact same concentrations of Q . Given the decomposition issues consistently observed with $\text{Pt}(\text{pop-BF}_2)^4$ over the course of time-resolved laser experiments, a complete set of data is not available at this time. That said, $\text{Pt}(\text{pop-BF}_2)^4$ in the presence of amine-type quenchers (as presented in section 3.3) exhibits classic Stern-Volmer-type dynamic quenching behavior of the triplet state. Additional research in this area could lend valuable insight to the mechanism of combined static and dynamic quenching of both the singlet and triplet states of $\text{Pt}(\text{pop-BF}_2)^4$ in the presence of metal complexes like $\text{Co}(\text{bpy})_3^{2+}$.

3.6 Materials and methods

Unless otherwise noted, all reagents were obtained from Sigma-Aldrich and used without further purification; all water used was deionized. All manipulations involving $\text{Pt}(\text{pop-BF}_2)^4$ were carried out with standard air-free techniques in an inert-atmosphere glovebox or utilizing a vacuum manifold. Solvents were dried using activated alumina columns according to Grubbs'

method.²⁰ Anhydrous acetonitrile was stored over activated 3 Å molecular sieves; all other anhydrous solvents were stored over activated 4 Å molecular sieves.²¹ Molecular sieves were activated by heating to 200 °C under reduced pressure for 4 hours.

3.6.1 $[Co(bpy)_3](PF_6)_2$ ^{22,23}



$Co(bpy)_3Cl_2$ was formed by mixing a solution of 3.27 g 2,2'-bipyridine in 100 mL methanol with a solution of 1.66 $CoCl_2 \cdot 6H_2O$ in 50 mL methanol and stirring for one hour. 11.4 g NH_4PF_6 was added to precipitate 8.3 g of a light yellow solid. This product was dissolved in 150 mL CH_2Cl_2 and filtered to remove ~2g residual NH_4Cl and NH_4PF_6 as a yellowish-white powder. The mother liquor was reduced in volume via rotary evaporation to yield shiny orange microcrystalline needles, which were rinsed with diethyl ether and dried under vacuum. Further purification may be achieved by recrystallization from acetone/methanol.

3.6.2 Steady-state quenching experiments

Steady-state emission spectra were recorded on a Jobin Yvon Spex Fluorolog-3-11. A 450-W xenon arc lamp was used as the excitation source with a single monochromator providing wavelength selection. Right-angle light emission was sorted using a single monochromator and fed into a Hamamatsu R928P photomultiplier tube with photon counting. Short and long pass filters were used where appropriate. Spectra were recorded on Datamax software.²

3.6.3 *Time-resolved quenching experiments*

To monitor singlet and triplet emission, samples were excited at 355 nm with 8-ns pulses from the third harmonic of a Q-switched Nd:YAG laser (Spectra-Physics Quanta-Ray PRO-Series) operating at 10 Hz. Emission wavelengths were selected using a double monochromator (Instruments SA DH-10) with 1 mm slits. Luminescence was detected with a photomultiplier tube (PMT, Hamamatsu R928). The PMT current was amplified and recorded with a transient digitizer (Tektronix DSA 602). Short- and long-pass filters were employed to remove scattered excitation light. Decay traces were averaged over 500 laser pulses. Instruments and electronics in this system were controlled by software written in LabVIEW (National Instruments). Data manipulation was performed and plotted using MATLAB R2015a (Mathworks, Inc.).²

REFERENCES

- (1) Lakowicz, J. R. *Principles of Fluorescence Spectroscopy*; Springer US, 2006.
- (2) Durrell, A. C.; Keller, G. E.; Lam, Y.-C.; Sykora, J.; Vlček, A.; Gray, H. B. *J. Am. Chem. Soc.* **2012**, *134*, 14201.
- (3) Vogler, A.; Kunkely, H. *Angewandte Chemie International Edition in English* **1984**, *23*, 316.
- (4) Alexander, K. A.; Bryan, S. A.; Dickson, M. K.; Hedden, D.; Roundhill, D. M.; Che, C. M.; Butler, L. G.; Gray, H. B. In *Inorganic Syntheses*; John Wiley & Sons, Inc.: 1986; Vol. 24, p 211.
- (5) Che, C. M.; Butler, L. G.; Grunthaner, P. J.; Gray, H. B. *Inorg. Chem.* **1985**, *24*, 4662.
- (6) Che, C. M.; Butler, L. G.; Gray, H. B. *J. Am. Chem. Soc.* **1981**, *103*, 7796.
- (7) Che, C. M.; Butler, L. G.; Gray, H. B.; Crooks, R. M.; Woodruff, W. H. *J. Am. Chem. Soc.* **1983**, *105*, 5492.
- (8) Stiegman, A. E.; Rice, S. F.; Gray, H. B.; Miskowski, V. M. *Inorg. Chem.* **1987**, *26*, 1112.
- (9) Vlček, A.; Gray, H. B. *J. Am. Chem. Soc.* **1987**, *109*, 286.
- (10) Smith, D. C.; Gray, H. B. *Coord. Chem. Rev.* **1990**, *100*, 169.
- (11) Sweeney, R. J.; Harvey, E. L.; Gray, H. B. *Coord. Chem. Rev.* **1990**, *105*, 23.
- (12) Roundhill, D. M.; Gray, H. B.; Che, C. M. *Acc. Chem. Res.* **1989**, *22*, 55.
- (13) Lam, Y.-C.; Darnton, T. Unpublished results.
- (14) Harvey, E. L. Dissertation (Ph.D.), California Institute of Technology, 1990.
- (15) Lam, Y.-C., Caltech, 2015.
- (16) Fox, L. S.; Kozik, M.; Winkler, J. R.; Gray, H. B. *Science* **1990**, *247*, 1069.
- (17) Marcus, R. A. *The Journal of Chemical Physics* **1956**, *24*, 966.
- (18) Marcus, R. A. *J. Phys. Chem.* **1963**, *67*, 853.
- (19) Darnton, T. V.; Hunter, B. M.; Hill, M. G.; Záliš, S.; Vlček, A.; Gray, H. B. *J. Am. Chem. Soc.* **2016**, *138*, 5699.
- (20) Pangborn, A. B.; Giardello, M. A.; Grubbs, R. H.; Rosen, R. K.; Timmers, F. J. *Organometallics* **1996**, *15*, 1518.
- (21) Armarego, W. L. F.; Chai, C. L. L. In *Purification of Laboratory Chemicals (Sixth Edition)*; Butterworth-Heinemann: Oxford, 2009, p 88.
- (22) Hamann, T. W.; Gstrein, F.; Brunschwig, B. S.; Lewis, N. S. *J. Am. Chem. Soc.* **2005**, *127*, 13949.
- (23) Feldt, S. M.; Gibson, E. A.; Gabrielsson, E.; Sun, L.; Boschloo, G.; Hagfeldt, A. *J. Am. Chem. Soc.* **2010**, *132*, 16714.